Published in final edited form as:

Anat Rec (Hoboken). 2020 June ; 303(6): 1717–1726. doi:10.1002/ar.24393.

Endothelial – Stromal Communication in Murine and Human Corneas

Lauren Jeang[2], **Byeong J Cha**[1], **David E Birk**[1], **Edgar M Espana**[1,2]

[1]Department of Molecular Pharmacology & Physiology, Morsani College of Medicine, University of South Florida, Tampa, Florida

[2]Cornea, External Disease and Refractive Surgery, Department of Ophthalmology, Morsani College of Medicine, University of South Florida, Tampa, Florida

Abstract

The purpose of this study is to identify and characterize interactions of corneal endothelial cells with the underlying posterior stroma. Corneal endothelial - stromal interactions were defined in developing postnatal day 3 (P3) and maturing and postnatal day 30 (P30) C57BL/6 mice as well as in adult human corneas. Flat mounts and cross sections were studied using immunofluorescence microscopy from and postnatal day 30 (P30). F-actin was localized using phalloidin to evaluate cell processes traversing Descemet's membrane (DM). Dynamic cell - cell communication was evaluated by analyzing the pattern of fluorescence recovery using calcein AM dye transfer after selective photo-bleaching. Endothelial - stromal interactions, seen along Descemet's membrane (DM) during development (P3), were only found in the periphery of the mature murine cornea (P30). In mature human corneas, cellular extensions through the DM were noted in the peripheral cornea. The pattern of fluorescence recovery after photo-bleaching in both mature mice and human central corneas demonstrated endothelial - endothelial cell communication. In contrast, in the human cornea 2 distinct patterns were observed consistent with endothelial - endothelial as well as stromal - endothelial communication. Endothelial - stromal interactions are present in the entire cornea during early postnatal life. Endothelial-stromal interactions localize to the periphery of the cornea in the adult. The existence of direct endothelial – posterior stromal contact contradicts the conception that corneal endothelial cells are isolated from the stroma by the DM and implies that endothelial - stromal comunication can influence corneal structure and function.

Keywords

Cornea; endothelium; stroma; Descemet's membrane; fluorescence recovery; cellular communication

Address correspondence, proof, and reprint requests to: Edgar M Espana, M.D. University of South Florida Eye Institute, Department of Molecular Pharmacology & Physiology, Morsani College of Medicine, Tampa, FL 33612 Tel: 813 974 1981 eespana@usf.edu.

Proprietary Interests: None.

INTRODUCTION

The corneal endothelium is a monolayer of neural crest derived cells responsible for maintaining the appropriate degree of corneal stroma hydration necessary for transparency (Waring et al., 1982; Tuft and Coster, 1990; Edelhauser, 2006). Loss of corneal endothelial cells below a critical number is associated with stromal swelling, epithelial blistering and decreased vision (Mishima, 1982; Edelhauser, 2006). Endothelial cell counts below 300–500 cells per mm^2, are associated with irreversible corneal swelling and need of endothelial replacement in humans (Mishima, 1982; Edelhauser, 2006). Multidirectional interactions between the corneal endothelium and the posterior stroma would provide a mechanism for the collective regulation of corneal structure and function.

Previous work suggests that endothelial cells interact directly with the underlying stroma (Cintron et al., 1988; Fitch et al., 1990; Hemmavanh et al., 2013). Direct stroma – endothelial cell connections and the presence of pores in Descemet's membrane (DM) in the developing rabbit cornea is suggestive of direct endothelial – stromal cell interaction (Cintron et al., 1988). Similarly, the presence of collagen IV- rich matrix penetrating the DM and connecting endothelial cells with the stroma at regular intervals in the chicken cornea was demonstrated (Fitch et al., 1990). We also demonstrated DM pores indicative of endothelial – stromal communication in the mouse cornea (Hemmavanh et al., 2013). Although the implications of such findings are unknown, the presence of direct endothelial – stromal contact contradicts the dogma that endothelial cells are isolated from the stroma by the DM and, most importantly, rises the possibility that stromal - endothelial interactions have a role in influencing structure and function.

To analyze potential endothelial – stromal comunication, we used complementary approaches; morphological analyses using confocal imaging, and functional analyses using fluorescence recovery after photobleaching (FRAP) assays (Wade et al., 1986). We used calcein AM, a cell-permeant dye, electrically neutral and highly lipophilic molecule, that can permeate rapidly into the cytoplasm through gap junctions (Kuzma-Kuzniarska et al., 2014) and is used to determine cell viability in eukaryotic cells including human and murine corneal cells (Poole et al., 1993; Espana et al., 2003; Kawakita et al., 2005). In live cells, non-fluorescent calcein AM is converted to a green-fluorescent calcein after acetoxymethyl ester hydrolysis by intracellular esterases (Bell et al., 1988). FRAP is a technique widely used to study molecule transport, diffusion, interaction, and immobilization in live cells (Peters et al., 1974; Axelrod et al., 1976; Houtsmuller, 2005). FRAP experiments are based on photo-bleaching a fluorescent marker in a selected area, followed by relaxation back to equilibrium (Peters et al., 1974; Phair and Misteli, 2001). It involves 3 steps: pre-bleaching targeted cells - to record the fluorescent intensity baseline; a bleaching sequence of targeted cells; and a post-bleaching image sequence to record the entry of fluorescent molecules from surrounding cells. Using this approach, functional cell communication can be demonstrated by dye transfer. Our results demonstrate the presence of anatomical and functional interactions between the corneal endothelium and the posterior stroma in mouse and in human eyes. There are spatial changes in their localization during development. Anatomical interactions present across the cornea early in development become restricted to the peripheral cornea with maturation.

MATERIALS AND METHODS

Human Tissue

Fresh human corneoscleral tissue (n=6) preserved in storage medium (Optisol; Chiron Vision, Irvine, CA) and not suitable for transplantation was obtained. Corneal tissue from 49 to 70-year-old donors, mean age 61.3 ± 10.9 years were kindly provided by the Tampa Lions Eye Bank (Tampa, FL) and managed in accordance with the Declaration of Helsinki. Corneas were precut using a Moria microkeratome (Doylestown, PA, USA) at a depth of approximately 400 – 450 μm. The corneas were immediately preserved in Optisol GS preservation medium and used within 24 hours. The posterior stroma and DM/endothelial cells complex with an approximate thickness of 100 μm was used for experiments after removing an anterior stromal cap. A thinner posterior stroma and DM/endothelial cells complex was easier to flatten under the microscope and be evaluated with microscopy.

Animals

C57BL/6 (Charles River) mice were used in this study. Corneal tissue from mice at postnatal day 3 (P3) n=6 and postnatal day 30, (P30) n=12 were examined. All experiments conformed to the use of Laboratory Animals and ARVO statement for the Use of Animals in Ophthalmic and Vision Research and were approved by the Institutional Animal Care and Use Committee of the University of South Florida, College of Medicine.

Immunofluorescence in Frozen Corneal Cross Sections

Immunofluorescence analysis was performed as previously described (Hemmavanh, Koch, Birk and Espana, 2013; Sun et al., 2011). Corneal tissue was prepared for examination as cross-sections. Briefly, corneas were embedded and snap frozen in OCT medium (Sakura Finetek, Torrance, CA). Cross sections of 5 μm were cut using a HM 505E cryostat. Sections were fixed in acetone for 5 minutes at 4ºC. Human and murine corneal sections were blocked using 5% bovine serum albumin (BSA) and incubated with Alexa Fluor 594 phalloidin (Molecular Probes) overnight. In some sections, antibody against collagen IV was used at a 1:100 dilution (Southern Biotechnology, Alabama, USA) followed by incubation with Alexa Fluor 594 phalloidin. A donkey anti-goat antibody was used as secondary antibody (Molecular probes, Thermo Fisher, USA). Descemet's membrane was used as positive control for collagen IV staining and negative controls were processed only with PBS. The nuclei were counterstained using Vectashield mounting solution with DAPI (Vector Lab Inc., Burlingame, CA). Images were captured using a confocal laser-scanning microscope (FV1000 MPE; Olympus) and a Leica fluorescent microscope with either a 40X (0.75 NA) or a 60X (1.42 NA) oil immersion objective lens. To avoid bleed through between fluorescence emissions, samples were scanned sequentially with 488- and 590-nm lasers, and emissions were collected with appropriate spectral slit settings.

Immunofluorescence in Flat Mount Preparations

Freshly harversted murine globes were dissected under a dissecting microscope (Zeiss, Germany) and sclerocorneal rims prepared for flat mount examination. Flat mounts were fixed in acetone for 5 minutes at 4ºC and blocked in 5% bovine serum albumin (BSA) and

incubated with Alexa Fluor 594 phalloidin overnight. Tissue was processed and stained as above. Z-Pack images were obtained of the posterior stroma and endothelium using a confocal laser-scanning microscope (FV1000 MPE; Olympus America, Inc., Center Valley, PA, USA) with a 60 x lens. For stromal cell density calculations, keratocyes located immediately under DM were counted in each photograph by objectively counting the number of DAPI stained nuclei using Image J open source software (national Institute of Health, Bethesda, USA) that thresholded the nuclei objectively in images obtained at 60x magnification. Cell nuclei were counted in 4 different locations. Data was obtained from 3 different biological replicates.

Fluorescence Recovery after Photobleaching (FRAP) in Calcein Loaded Corneal Cells

Freshly enucleated mouse corneas that included a small segment of sclera or human sclerocorneal precut tissue after removal of the anterior stromal cap were placed in a solution containing 1μm calcein AM (Becton Dickinson and Company, Franklin Lakes, NJ) in phenol red free DMEM (Life technologies). The segments were incubated for 15 minutes and then washed 3 times in phenol red free DMEM. Flat corneoscleral mounts were then prepared by placing the tissue endothelial side face down on a coverslip that was covered with phenol red free DMEM. Corneal endothelial cells were observed using a 3i spinning disk confocal imaging system (Intelligent Imaging Innovations) mounted on an Olympus IX81 inverted microscope with 20x (0.75NA) objective. A circular region of interest in the endothelial monolayer was photo-bleached using 488 nm point laser scanning for 5 seconds. The recovery of fluorescence was recorded at 1 second intervals and the relative intensity and pattern of fluorescence recovery in 2 different locations within the circular region of interest: center and outer circumference within the bleached area, were analyzed using Slidebook 5.0 software (3i, Denver, CO). Three to five different areas in the peripheral cornea, area located in the transition zone to the sclera, and 3 – 5 in the central cornea were evaluated per eye and the best quality captures recorded as a video. Ten murine P30 corneas and 6 human corneas were used and video recording of the experiment was obtained. Image J open source software was used to measure fluorescence intensity, in the recorded videos, at different times following photobleaching in the 2 different locations within the photobleached circular region. Cell fluorescence was continuously measured for at least 100 seconds in all samples.

Statistical Analysis

Data obtained from saved images from the posterior cornea and recorded videos from central and peripheral cornea were reviewed for statistical analyses. Nuclei density (cells per 60x mag field) at P3 and P30 were obtained from Image J software. Mean and Standard Deviation (SD) were obtained and compared using student’s paired t-test. The Delta obtained between the initial fluorescence intensity measured in the center and outer circumference immediately after photo-bleaching and the final fluorescence intensity recovered after 100 seconds was analyzed in the central and peripheral cornea. Mean fluorescence, SD and rate of fluorescence recovery obtained from different samples were compared using student’s unpaired t-test. $p<0.05$ was considered statistically significant. All statistical analysis were performed using GraphPad Prism, (GraphPad Software Inc, San Diego, California, USA).

RESULTS

Murine Corneal Endothelial – Stromal Interactions and Subendothelial Keratocyte Density Decrease During Corneal Maturation

Extensive endothelial cell processes projecting anteriorly through the DM were observed in the P3 immature mouse cornea after cytoplasmic fibrillar actin staining with fluorescently conjugated phalloidin. These processes suggest a potential for functional and physical cell-cell communication between endothelial cells and underlying keratocytes. These endothelial processes were seen in the P3 central cornea as well as in the corneal periphery. Some endothelial cells had multiple cell processes that communicate with underlying keratocytes (Fig. 1A,B). In contrast, in mature P30 corneas, endothelial cell processes interacting with the underlying stromal cells are only observed at the corneal periphery (Fig. 1C).

A decrease in endothelial - stromal communication also correlates with a decrease in the density of posterior stromal keratocytes. A dense network of keratocytes in the posterior stroma, adjacent to the DM and endothelium is present in the immature central cornea at P3 (Fig. 2C). The density of the keratocyte in the mature P30 central cornea (Fig. 2F) decreased significantly compared to the P3 cornea, (Fig. 2C), 10.3 ± 1.2 vs 13.2 ± 1.9 nuclei per 60x field, statistically significant difference, $p=0.016$.

Murine Endothelial Cell – Stromal Cell Communication is Restricted to the Peripheral Mature Cornea

Functional cell-cell communication in the central and peripheral murine cornea was evaluated using FRAP. A predetermined circular area of endothelial cells that have been preloaded with calcein AM was photo-bleached. In the central cornea, laser scanning confocal microscopy showed fluorescence recovery that progressed from endothelial cells in the outer circumference of the bleached circle to endothelial cells in the center of the circle. The recovery of cell fluorescence started in the outer circumference, and the intensity of fluorescence was stronger in the outer circumference compared to the center (Fig. 3). The rate of fluorescence recovery was faster in the outer circumference compared to the center of the bleached circle at 10 secs (1.76 vs 1.55) and continued to be faster at 100 second (Table 1). This is consistent with predominantly endothelial-endothelial cell dye transfer in the central cornea where we did not find structural endothelial-stromal cell interactions. In contrast, fluorescence recovery in the peripheral cornea showed a different fluorescence recovery pattern. Calcein fluorescence recovery began simultaneously at the center and at the outer circumference of the photo-bleached circle (Fig. 4). The rate of fluorescence recovery was faster in the center compared to the outer circumference at 10 seconds (2.36 vs 2.12) and continued to be faster at 100 seconds (Table 1). However, Delta obtained between the initial fluorescence intensity measured in the central and peripheral cornea immediately after photo-bleaching and the final fluorescence intensity recovered after 100 seconds was not statistically significant, unpaired t-test, $p= 0.3125$. Together, these findings are suggestive of endothelial – endothelial cell communication in the central cornea. In contrast, in the peripheral cornea the pattern of fluorescence recovery is suggestive of the presence of communication between endothelial cells and the underlying stromal cells as well as endothelial to endothelial cells.

Adult Human Endothelial Cell – Stromal Keratocyte Communication is Restricted to the Peripheral Cornea

Endothelial cell processes consistent with physical interaction and communication of endothelial cells with underlying keratocytes were seen only in the peripheral adult human cornea in one sample (Fig. 5). In the peripheral human cornea, endothelial cell processes were observed traversing the DM (Fig. 5A-C). Traversing endothelial processes were not seen in the central cornea (Fig. 5D). Together, these findings suggest that endothelial-stromal interactions localize exclusively to the corneal periphery in the adult human cornea and are comparable to those in the murine cornea.

Similar to murine corneas, the pattern of fluorescence recovery in the human central cornea differed from that in the peripheral cornea. In the central cornea, cell fluorescence recovered first in endothelial cells located in the outer circumference of the photo-bleached circular area. Endothelial cells at the center of the bleached circle displayed significantly slower fluorescence recovery (Fig. 6). The rate of fluorescence recovery was faster in the outer circumference compared to the center of the bleached circle at 10 secs (0.90 vs 0.72) and continued to be faster at 100 seconds (Table 2). In contrast, fluorescence recovery in the peripheral cornea showed a different pattern. In some areas, almost simultaneous recovery of fluorescence was noted in the central and peripheral endothelial cells (Fig. 7), while in others peripheral areas, the pattern of fluorescence recovery was similar to that noted in the central cornea. The rate of fluorescence recovery was faster in the center compared to the outer circumference of the bleached circle at 10 secs (1.76 vs 1.47) and continued to be faster at 100 seconds (Table 2). Delta obtained between the initial fluorescence intensity measured in the human central and peripheral cornea immediately after photo-bleaching and the final fluorescence intensity recovered after 100 seconds was statistically significant, $p= 0.0296$, unpaired t-test, suggesting a significant difference in fluorescence recovery between central and peripheral areas of the cornea. Although, we noted a similar difference in fluorescence recovery between central and peripheral areas of the murine cornea. That difference did not reach statisticaly significance (Fig. 8). Together, these findings suggest that endothelial - keratocyte communication occurs only in the peripheral cornea.

DISCUSSION

In the current study, we find physical interactions between corneal endothelial cells and the underlying stroma in both mouse and human corneas. These interactions, present along the DM in the developing murine cornea, become localized to the peripheral cornea of the mature murine cornea. The adult human cornea is comparable to the mature murine cornea, in that endothelial-stromal interactions are confined to the peripheral cornea. This is consistent with previous work indicative of endothelial and stromal interactions in different species (Cintron et al., 1988; Fitch et al., 1990; Hemmavanh et al., 2013).

Once we determined the physical presence of endothelial – stromal interactions, our next approach was to determine if such interactions were functional. We used calcein AM to evaluate cell – cell communication. Calcein has a high retention rate within cells and high resistance to fluorescent quenching. Moreover, corneal endothelial preparations required no special incubation techniques before examination, which reduced artefacts and revealed the

delicate endothelial network alive and intact. To our knowledge this relatively simple technique has not previously been used to study the corneal endothelial communication in vivo, an application to which they appeared uniquely suited because the cornea's inherent transparency that can be utilized to image the undisturbed cells within the 3-dimensional stromal matrix.

The presence in the peripheral corneal of functional communication within neighboring endothelial cells and the underlying stromal keratocytes is supported by our FRAP analysis demonstrating transfer from the underlying stroma as well as from endothelial cells adjacent to the photo-bleached region. Based on our structural demonstration of endothelial – keratocyte interaction, we hypothesized functional communication between stromal and endothelial cells in the cornea which is supported by the FRAP data. In addition, the difference noted in the fluorescein recovery pattern between central and peripheral cornea is consistent with the changing distribution of endothelial-stromal interactions with maturation.

Corneal endothelial cells are known to communicate via gap junctions (Raviola et al., 1980; Watsky and Rae, 1992; Joyce et al., 1998).Transfer of dye from endothelial cells directly to the next endothelial cells is consistent with the central corneal data from mature mice where no endothelial-stromal interactions were observed. In contrast, the pattern of fluorescence recovery noted in the peripheral cornea of adult mice where endothelial-stromal interactions were observed differs from the central cornea and is consistent with dye transfer from keratocytes in the stroma to endothelial cells as well as endothelial cells directly to the next endothelial cell. Recovery of fluorescence does not start at the outer circumference of the bleached circle but at the center and is followed by the outer circumference of the bleached circular area. However, we cannot rule out that idiopathic or unknown differences in endothelial function or the technique are responsible for the different pattern noted with FRAP. The comparable data obtained using mature mice and human corneas support functional endothelial-stromal communication as a general mechanism with the potential to influence cell behavior in the endothelium and posterior corneal stroma.

It is unknown what effects endothelial-stromal interactions have on corneal development and function. We have previously shown that corneal endothelial maturation is delayed in *Col12a1*$^{-/-}$ and *Col14a1*$^{-/-}$ mouse models (Hemmavanh et al., 2013). This alteration of collagen XII and XIV, expressed in the posterior stroma, influences endothelial development and function. These data with our demonstration of changing patterns of endothelial-stromal communication in murine and human corneas suggest transduction of signals in the posterior stroma that can influence endothelial function. Previous work in humans and mice suggest that endothelial progenitor cells probably localize to the peripheral cornea. Hara et al shown enrichment of p75NTR (neurotrophin receptor) positive cells at the corneal endothelial side of the transition region between the corneal endothelium and the trabecular meshwork, however, no statistically significant difference was found neither in colony forming efficiency or number of p75NTR positive cells (Hara et al., 2014). He et al also demonstrated the presence of less differentiated cells as well as expression of stem cell markers in an area they refer to the extreme corneal endothelial periphery (He et al., 2012; Katikireddy et al., 2016). Our laboratory found the presence of slow cycling cells in the murine endothelial extreme periphery (Espana et al., 2015). We hypothesize that these

endothelial - stromal interactions may somehow be indicative of the location of an endothelial niche. It is provoking to hypothesize that the mature posterior cornea has a unique niche in the periphery where progenitor cells reside and that localization of endothelial-stromal interactions points to the location of such a niche.

In conclusion, we demonstrated physical endothelial cell-keratocyte interactions as well as functional communication in both murine and human corneas. In addition, the process of corneal endothelial maturation in murine corneas includes restriction of endothelial – stromal connections to the peripheral cornea. These findings support the presence of a niche in the periphery of the adult cornea with maintenance of functional communication in this region. Unveiling the mechanisms that regulate the structure and function of the endothelial niche open multiple translational opportunities to prevent corneal diseases, to improve corneal transplant survival and propose new surgical therapies.

Acknowledgments

Supported by: An unrestricted research grant from the Department of Ophthalmology, University of South Florida and NIH/NEI grant EY029395.

LITERATURE CITED

Axelrod D, Koppel DE, Schlessinger J, Elson E, Webb WW. 1976. Mobility measurement by analysis of fluorescence photobleaching recovery kinetics. Biophys J 16:1055–1069. [PubMed: 786399]

Bell RS, Bourret LA, Bell DF, Gebhardt MC, Rosenberg A, Berrey HB, Treadwell BV, Tomford WW, Mankin HJ. 1988. Evaluation of fluorescein diacetate for flow cytometric determination of cell viability in orthopaedic research. J Orthop Res 6:467–474. [PubMed: 3164067]

Cintron C, Covington HI, Kublin CL. 1988. Morphogenesis of rabbit corneal endothelium. Curr Eye Res 7:913–929. [PubMed: 3180839]

Edelhauser HF. 2006. The balance between corneal transparency and edema: the Proctor Lecture. Invest Ophthalmol Vis Sci 47:1754–1767. [PubMed: 16638979]

Espana EM, He H, Kawakita T, Di Pascuale MA, Raju VK, Liu CY, Tseng SC. 2003. Human keratocytes cultured on amniotic membrane stroma preserve morphology and express keratocan. Invest Ophthalmol Vis Sci 44:5136–5141. [PubMed: 14638709]

Espana EM, Sun M, Birk DE. 2015. Existence of Corneal Endothelial Slow-Cycling Cells. Invest Ophthalmol Vis Sci 56:3827–3837. [PubMed: 26066751]

Fitch JM, Birk DE, Linsenmayer C, Linsenmayer TF. 1990. The spatial organization of Descemet's membrane-associated type IV collagen in the avian cornea. J Cell Biol 110:1457–1468. [PubMed: 2182654]

Hara S, Hayashi R, Soma T, Kageyama T, Duncan T, Tsujikawa M, Nishida K. 2014. Identification and potential application of human corneal endothelial progenitor cells. Stem Cells Dev 23:2190–2201. [PubMed: 24588720]

He Z, Campolmi N, Gain P, Ha Thi BM, Dumollard JM, Duband S, Peoc'h M, Piselli S, Garraud O, Thuret G. 2012. Revisited microanatomy of the corneal endothelial periphery: new evidence for continuous centripetal migration of endothelial cells in humans. Stem Cells 30:2523–2534. [PubMed: 22949402]

Hemmavanh C, Koch M, Birk DE, Espana EM. 2013. Abnormal corneal endothelial maturation in collagen XII and XIV null mice. Invest Ophthalmol Vis Sci 54:3297–3308. [PubMed: 23599329]

Houtsmuller AB. 2005. Fluorescence recovery after photobleaching: application to nuclear proteins. Adv Biochem Eng Biotechnol 95:177–199. [PubMed: 16080269]

Joyce NC, Harris DL, Zieske JD. 1998. Mitotic inhibition of corneal endothelium in neonatal rats. Invest Ophthalmol Vis Sci 39:2572–2583. [PubMed: 9856767]

Katikireddy KR, Schmedt T, Price MO, Price FW, Jurkunas UV. 2016. Existence of Neural Crest-Derived Progenitor Cells in Normal and Fuchs Endothelial Dystrophy Corneal Endothelium. Am J Pathol 186:2736–2750. [PubMed: 27639969]

Kawakita T, Espana EM, He H, Hornia A, Yeh LK, Ouyang J, Liu CY, Tseng SC. 2005. Keratocan expression of murine keratocytes is maintained on amniotic membrane by down-regulating transforming growth factor-beta signaling. J Biol Chem 280:27085–27092. [PubMed: 15908433]

Kuzma-Kuzniarska M, Yapp C, Pearson-Jones TW, Jones AK, Hulley PA. 2014. Functional assessment of gap junctions in monolayer and three-dimensional cultures of human tendon cells using fluorescence recovery after photobleaching. J Biomed Opt 19:15001. [PubMed: 24390370]

Mishima S 1982. Clinical investigations on the corneal endothelium-XXXVIII Edward Jackson Memorial Lecture. Am J Ophthalmol 93:1–29. [PubMed: 6801985]

Peters R, Peters J, Tews KH, Bahr W. 1974. A microfluorimetric study of translational diffusion in erythrocyte membranes. Biochim Biophys Acta 367:282–294. [PubMed: 4429678]

Phair RD, Misteli T. 2001. Kinetic modelling approaches to in vivo imaging. Nat Rev Mol Cell Biol 2:898–907. [PubMed: 11733769]

Poole CA, Brookes NH, Clover GM. 1993. Keratocyte networks visualised in the living cornea using vital dyes. J Cell Sci 106 (Pt 2):685–691. [PubMed: 8282773]

Raviola E, Goodenough DA, Raviola G. 1980. Structure of rapidly frozen gap junctions. J Cell Biol 87:273279.

Sun M, Chen S, Adams SM, Florer JB, Liu H, Kao WW, Wenstrup RJ, Birk DE. 2011. Collagen V is a dominant regulator of collagen fibrillogenesis: dysfunctional regulation of structure and function in a corneal-stroma-specific Col5a1-null mouse model. J Cell Sci 124:4096–4105. [PubMed: 22159420]

Tuft SJ, Coster DJ. 1990. The corneal endothelium. Eye (Lond) 4 (Pt 3):389–424. [PubMed: 2209904]

Wade MH, Trosko JE, Schindler M. 1986. A fluorescence photobleaching assay of gap junction-mediated communication between human cells. Science 232:525–528. [PubMed: 3961495]

Waring GO 3rd, Bourne WM, Edelhauser HF, Kenyon KR. 1982. The corneal endothelium. Normal and pathologic structure and function. Ophthalmology 89:531–590. [PubMed: 7122038]

Watsky MA, Rae JL. 1992. Dye coupling in the corneal endothelium: effects of ouabain and extracellular calcium removal. Cell Tissue Res 269:57–63. [PubMed: 1423485]

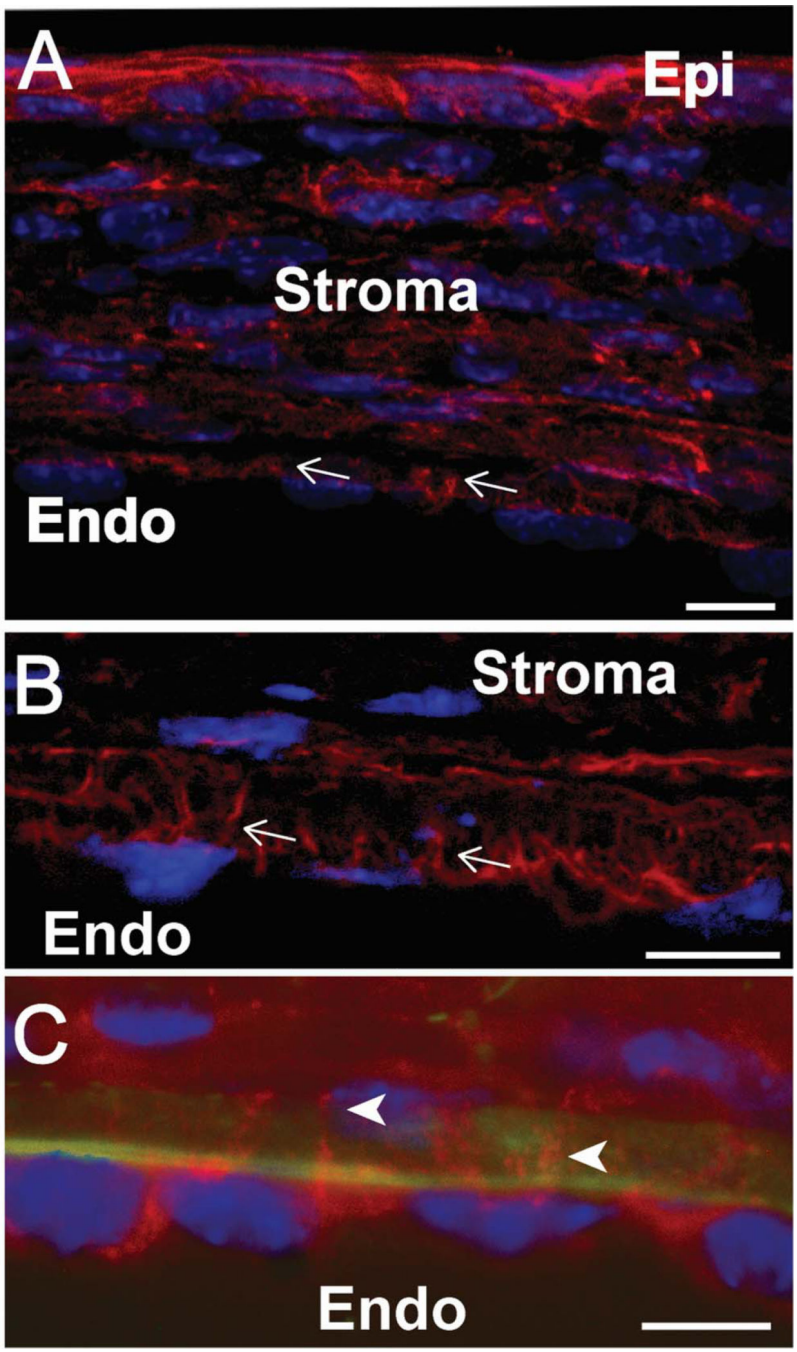

Figure 1. Endothelial – stromal communication are restricted to corneal periphery with corneal maturation.

(A) Phalloidin staining demonstrates endothelial - stromal processes suggestive of communication in the P3 cornea. (B) Higher magnification shows extensive cell communications at P3. (C) Stromal-endothelial communications are seen only in the corneal periphery at P30. White arrowheads point to cell processes. Green shows collagen IV in Descemet's membrane. Red shows F-actin processes and blue is cell nuclei demonstrated by DAPI staining. Representative micrographs are shown. Bar 10μm.

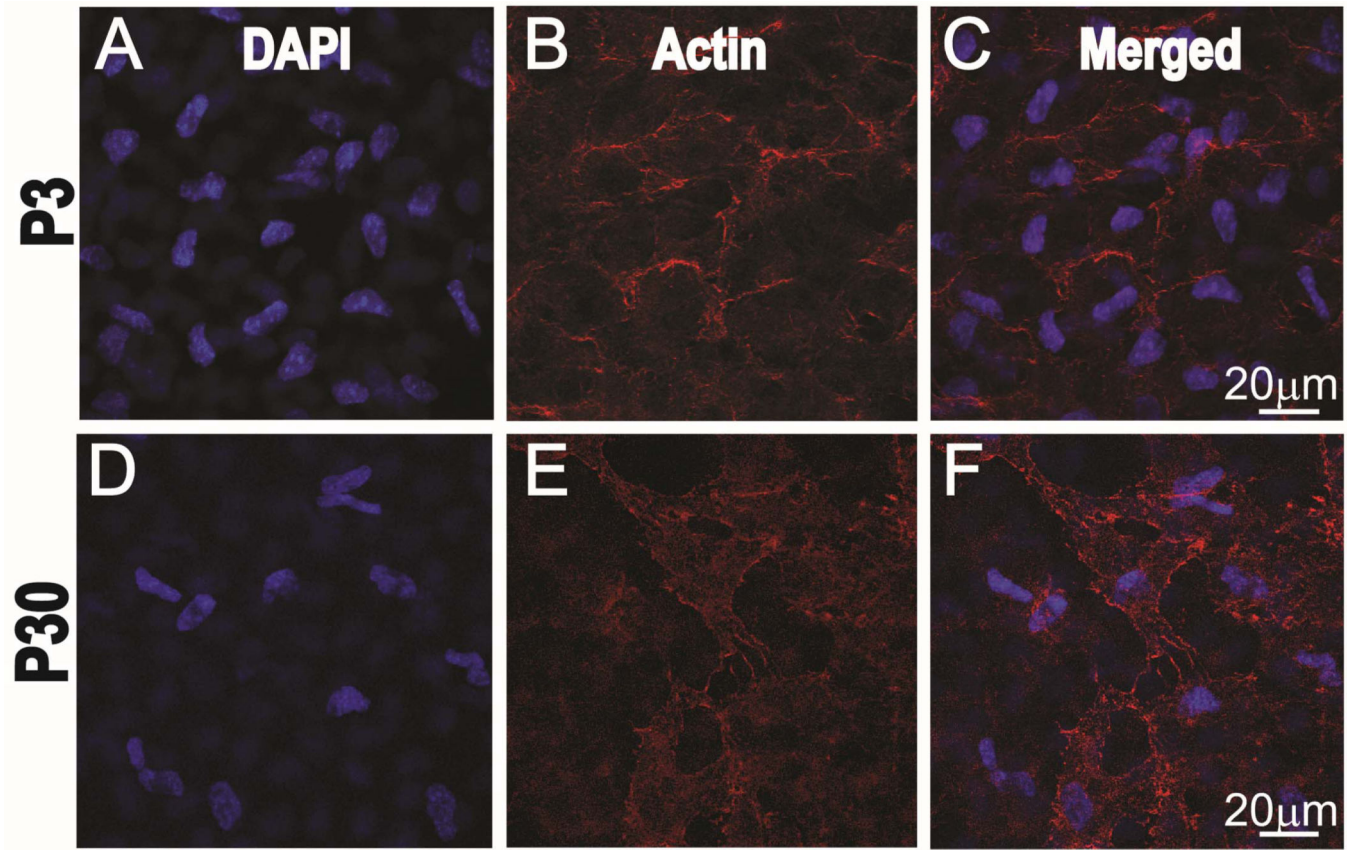

Figure 2. The density of subendothelial keratocytes decrease with corneal maturation.

Postnatal day 3 sub-endothelial keratocytes nuclei stained with DAPI, blue channel (A). F-actin staining of the cytoskeleton using phalloidin, red channel (B) and merged channels (C). Reduction in subendothelial keratocytes density is noted at postnatal day 30, Nuclei stained with DAPI, blue channel (D). F-actin staining of the cytoskeleton using phalloidin, red channel. (E) and merged channels (F). Representative micrographs are shown.

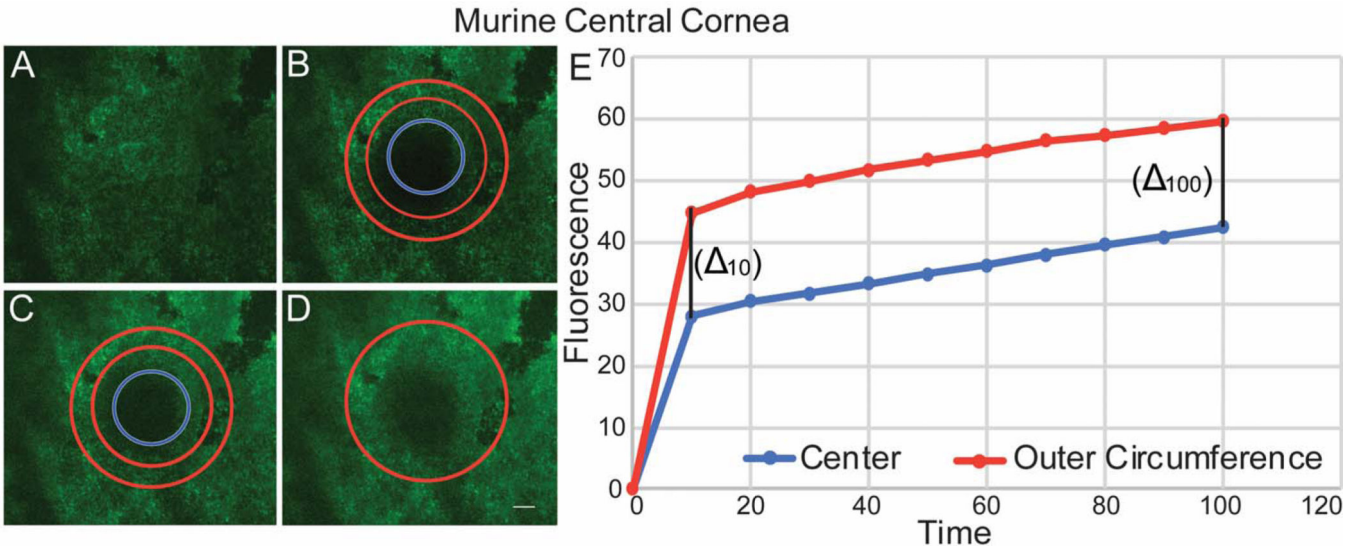

Figure 3. Endothelial – endothelial communications demonstrated by fluorescence recovery in the central cornea after photo-bleaching.

(A) Endothelial cells in the central cornea were uploaded with Calcein AM. (B) A circular area of the endothelial monolayer was photo-bleached. (C) The intensity of fluorescence recovery after photo-bleaching was evaluated at 2 different areas of the circle, center -blue circle- and outer circumference – red donut. (D) All bleached endothelial cells recover fluorescence at 100 seconds. (E) Graphic shows speed and pattern of fluorescence recovery in the central cornea. Note that endothelial cells in the periphery of the bleached circle recover fluorescence first, followed by the central endothelial cells with a similar fluorescence recovery rate demonstrated by a similar Delta between center and outer rim at 10 and 100 seconds. Note: a representative experiment is shown in this graphic. This image does not represent table 1.

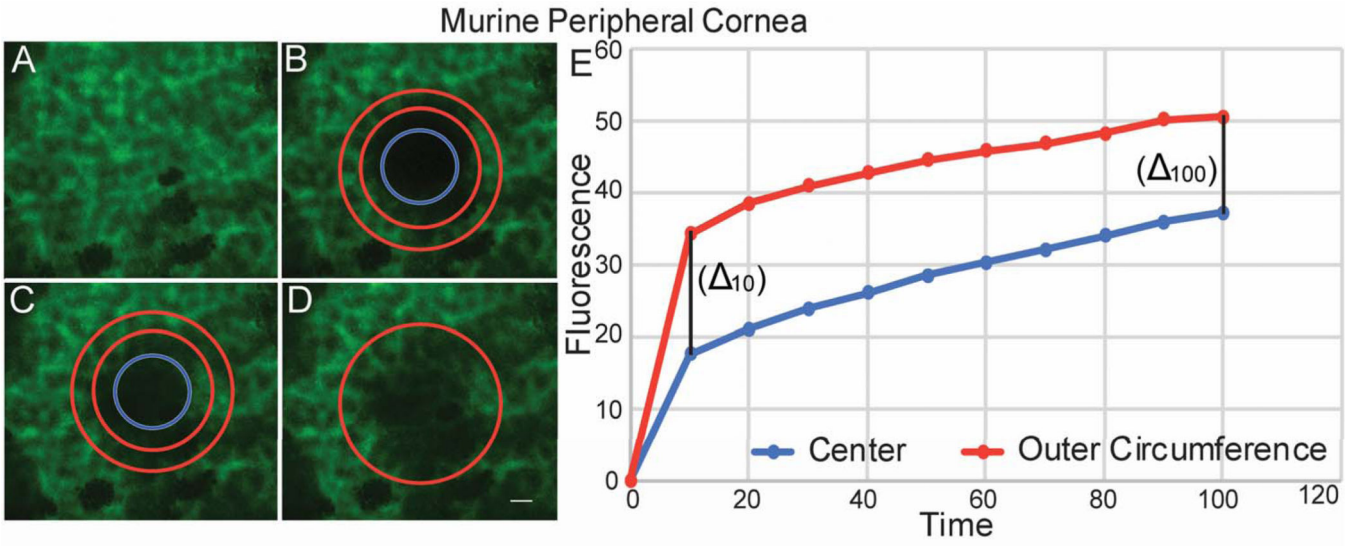

Figure 4. Endothelial – stromal communications demonstrated by Fluorescence Recovery in the Peripheral Cornea after photo-bleaching.

(A) Endothelial cells were uploaded with Calcein AM. (B) A circular area of the endothelial monolayer was photobleached. (C) The intensity of fluorescence recovery after photobleaching was evaluated at 2 different areas of the photobleached circle. (D) Endothelial cells recovered fluorescence at 100 seconds. (E) Graphic shows speed and pattern of fluorescence recovery in the peripheral cornea. Note that endothelial cells in the periphery of the bleached circle recover fluorescence first, followed by the central endothelial cells. There is a faster fluorescence recovery rate in the center area compared to the outer rim. The 2 lines are closer at 100 seconds. A representative experiment is shown. This image does not represent table 1.

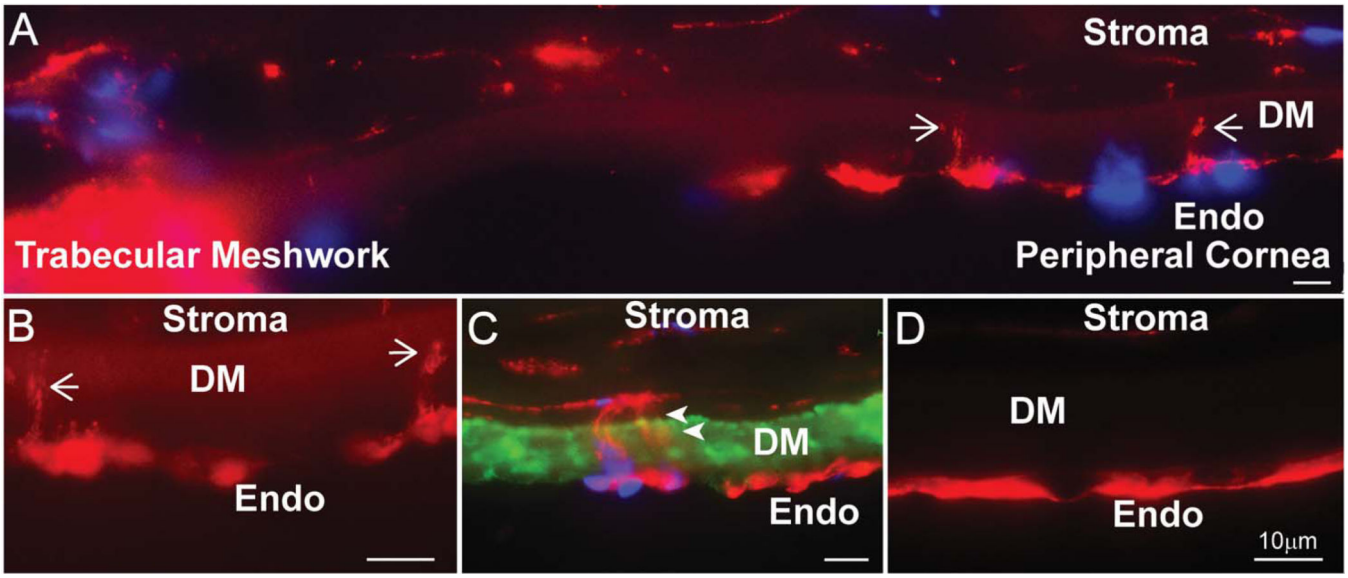

Figure 5. Endothelial-stromal processes are present in the peripheral human cornea.

(A) Composite image shows the human trabecular meshwork and peripheral cornea. Phalloidin staining shows F-actin cell processes crossing into DM, shown by white arrows. (B) Phalloidin staining shows actin cell processes penetrating DM at higher magnification. (C) Collagen IV staining of Descemet's membrane shows cell contacts between endothelial and stromal cells. White arrowheads (D) No cell processes are noted in the central cornea. Green represents collagen IV, red shows F-actin processes and blue is cell nuclei demonstrated by DAPI staining.

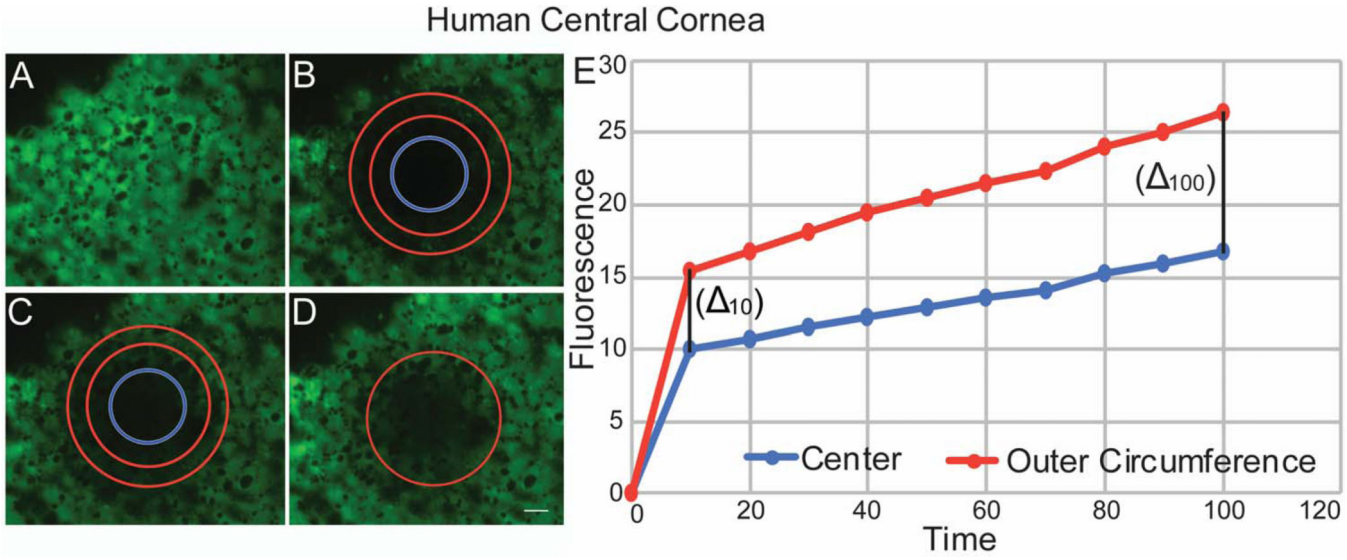

Figure 6. Endothelial – Endothelial Communications Demonstrated by Fluorescence Recovery in the Human Central Cornea after photo-bleaching.

(A) Human endothelial cells were uploaded with calcein AM. (B) A circular area of the endothelial monolayer was photo-bleached. (C) The intensity of fluorescence recovery after photobleaching was evaluated at the 2 different areas of the circle. (D) Endothelial cells recovered fluorescence at 100 seconds. (E) Graphic shows speed and pattern of fluorescence recovery in the central cornea similar to murine. Note that endothelial cells in the outer circumference of the bleached circle recover fluorescence first, followed by the central endothelial cells. This image does not represent table 2.

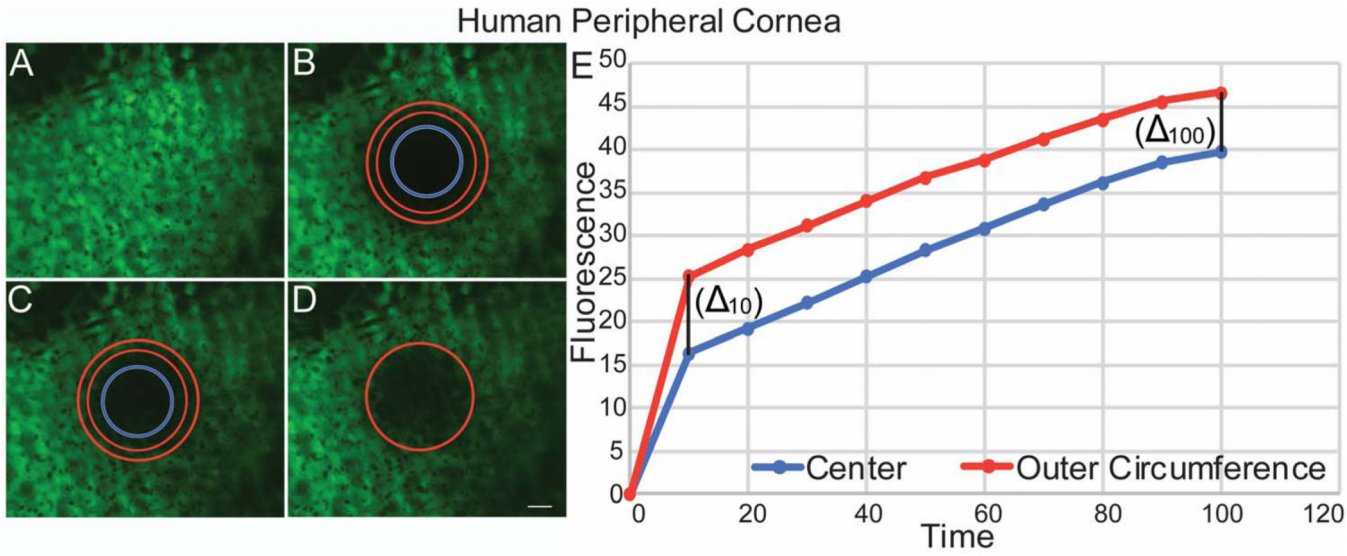

Figure 7. Endothelial – Stromal Communications demonstrated by Fluorescence Recovery in the Human Peripheral Cornea after photobleaching.

(A) Human endothelial cells were uploaded with calcein AM. (B) A circular area of the endothelial monolayer was photobleached. (C) The intensity of fluorescence recovery after photobleaching was evaluated at the 2 different areas of the circle, center and outer rim. (D) Endothelial cells recovered fluorescence at 100 seconds. (E) Graphic shows speed and pattern of fluorescence recovery in the peripheral cornea. Note that endothelial cells recover fluorescence in a pattern similar to murine peripheral cornea. A representative experiment is shown. This image does not represent table 2.

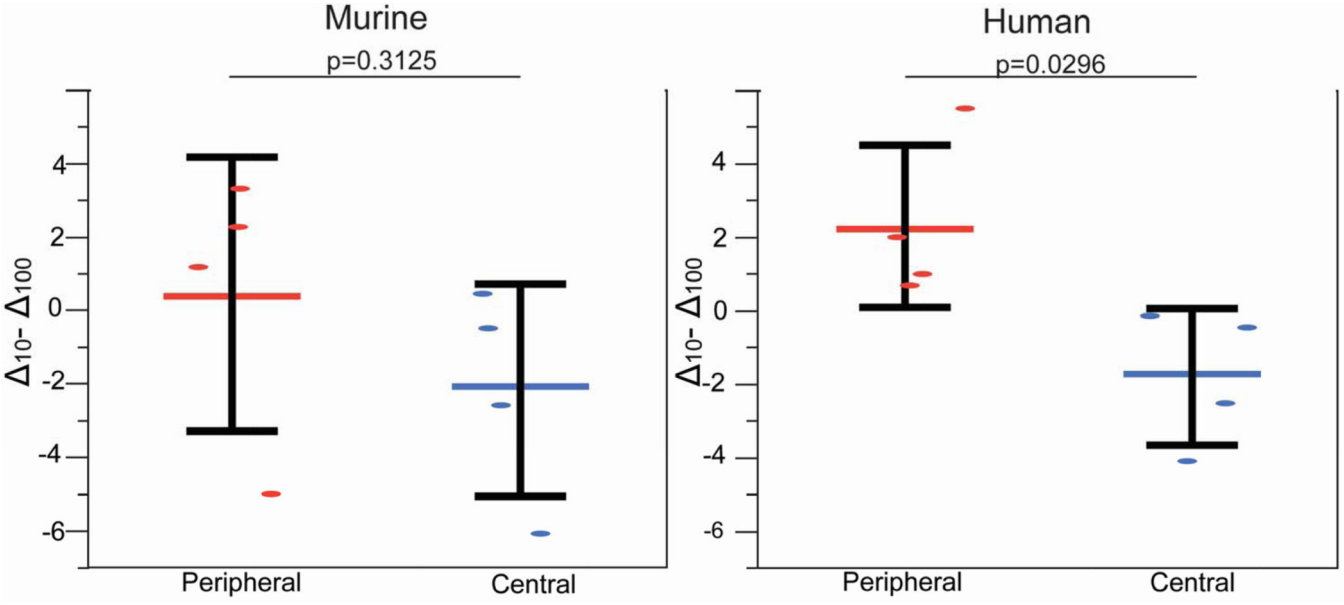

Figure 8. Difference in Fluorescence Recovery Rate at 10 and 100 secs (delta 10–100) obtained from center and outer rim of photobleached central and peripheral murine and human corneas.

Table 1.

Fluorescence intensity measurement and recovery rate following photobleaching in murine tissue.

	Central Cornea						Peripheral Cornea					
T	**Center**			**Outer Circumference**			**Center**			**Outer Circumference**		
(sec)	**Fluorescence Intensity (mean)**	**Fluorescence Intensity (SD)**	**Fluorescence Recovery Rate (intensit/sec)**	**Fluorescence Intensity (mean)**	**Fluorescence Intensity (SD)**	**Fluorescence Recovery Rate (intensit/sec)**	**Fluorescence Intensity (mean)**	**Fluorescence Intensity (SD)**	**Fluorescence Recovery Rate (intensit/sec)**	**Fluorescence Intensity (mean)**	**Fluorescence Intensity (SD)**	**Fluorescence Recovery Rate (intensit/sec)**
0	0	0	0	0	0	0	0	0	0	0	0	0
10	35.73	9.23	1.55	45.92	7.22	1.76	54.47	17.79	2.36	44.98	23.58	2.12
20	38.97	10.51	1.22	50.14	8.17	1.34	59.77	19.09	1.83	49.67	24.96	1.6
30	41.44	11.73	0.98	52.72	8.35	1.08	63.44	20.24	1.46	52.96	26.38	1.32
40	35.5	24.29	1.57	43.70	28.05	1.99	66.34	21.56	1.17	55.95	27.56	1.02
50	44.28	11.86	0.69	56.10	7.75	0.75	68.54	22.00	0.96	58.01	27.79	0.82
60	45.16	12.65	0.60	57.20	9.03	0.64	70.34	23.35	0.78	59.78	27.88	0.64
70	47.22	11.96	0.40	59.57	7.69	0.40	71.87	23.35	0.62	60.98	28.59	0.52
80	48.71	12.34	0.25	60.87	7.68	0.27	74.34	23.75	0.38	63.25	28.44	0.29
90	49.62	11.98	0.16	62.21	7.59	0.13	76.59	24.29	0.15	65.03	28.44	0.11
100	51.26	12.03	0.08	63.61	7.43	0.06	78.14	25.33	0.07	66.22	28.91	0.06

Table 2.

Fluorescence intensity measurement and recovery rate following photobleaching in human tissue.

	Central Cornea						Peripheral Cornea					
T	**Center**			**Outer Circumference**			**Center**			**Outer Circumference**		
(sec)	**Fluorescence Intensity (mean)**	**Fluorescence Intensity (SD)**	**Fluorescence Recovery Rate (intensit/sec)**	**Fluorescence Intensity (mean)**	**Fluorescence Intensity (SD)**	**Fluorescence Recovery Rate (intensit/sec)**	**Fluorescence Intensity (mean)**	**Fluorescence Intensity (SD)**	**Fluorescence Recovery Rate (intensit/sec)**	**Fluorescence Intensity (mean)**	**Fluorescence Intensity (SD)**	**Fluorescence Recovery Rate (intensit/sec)**
0	0	0	0	0	0	0		0	0	0	0	0
10	21.68	15.32	0.72	24.49	10.29	0.90	20.95	10.18	1.76	28.82	7.34	1.47
20	22.86	15.57	0.60	26.06	10.66	0.74	23.55	9.16	1.50	31.61	6.63	1.19
30	23.67	15.64	0.52	27.21	10.55	0.63	26.14	8.26	1.24	33.90	5.97	0.98
40	24.26	15.93	0.46	28.03	10.83	0.55	28.40	7.85	1.01	35.86	5.97	0.77
50	25.18	15.82	0.37	29.27	10.51	0.42	30.83	7.03	0.77	37.79	5.29	0.58
60	25.95	16.11	0.28	30.1	10.55	0.34	32.61	6.46	0.59	39.25	5.10	0.43
70	26.46	16.10	0.24	30.77	10.50	0.27	34.45	6.71	0.41	40.72	5.53	0.28
80	27.53	15.86	0.13	32.07	10.16	0.14	36.06	6.79	0.24	41.78	5.79	0.18
90	28.21	15.83	0.06	32.82	9.92	0.07	37.28	6.13	0.12	42.69	5.63	0.09
100	28.89	15.83	0.03	33.53	9.49	0.03	38.55	5.94	0.07	43.61	5.68	0.05